

## Ultrasonic Propagation in RbMnF<sub>3</sub>. II. Magnetoelastic Properties\*

R. L. MELCHER†

*Arthur H. Compton Laboratory of Physics, Washington University, St. Louis, Missouri 63130*

and

*Laboratory of Atomic and Solid State Physics, Cornell University, Ithaca, New York 14850*

AND

D. I. BOLEF

*Arthur H. Compton Laboratory of Physics, Washington University, St. Louis, Missouri 63130*

(Received 24 February 1969)

A study of the propagation of rf ultrasonic waves in the antiferromagnetically ordered state of RbMnF<sub>3</sub> is presented. Consideration of the effect of the sublattice magnetization orientation on the coupling between elastic and magnetic modes of the system results in the prediction of a strong magnetic field dependence of the measured elastic constants. Quantitative comparison with experiment is given, and the results are used to obtain values of the magnetoelastic coupling constants  $b_1$  and  $b_2$  and the anisotropy constant  $K$  at 4.2 K. The temperature dependence of the measured elastic constants, which show sharp anomalies at  $T \approx 60$  K, is readily explained with the present model.

### I. INTRODUCTION

IN a previous paper<sup>1</sup> (to be referred to as I), we presented the results of a study of the elastic properties of RbMnF<sub>3</sub> from 4.2 to 300 K. One of the results of this study was the observation of a very strong dependence of the "effective" or measured elastic constants  $C_{ij}$ \* on the orientation and magnitude of an applied magnetic field. This effect was observed only in the antiferromagnetically ordered state ( $T < T_N = 83$  K) and was strongly temperature-dependent.<sup>1,2</sup> The origin of this field dependence was discussed briefly (in I) in terms of a model in which the effective coupling of the elastic waves to the antiferromagnetic resonance modes is determined by the orientation in space of the sublattice magnetization vectors  $\mathbf{M}_i^0$  ( $i = 1, 2$ ); the orientation of these is dependent on the applied magnetic field  $\mathbf{H}_0$ . In the low-frequency limit (well satisfied in the present study) the measured "effective" elastic constants are independent of frequency, but depend on the applied magnetic field. The effect is a result of the field dependence of the effective coupling between the elastic and magnetic modes, and not a result of the field "tuning" the magnetic modes with respect to the elastic modes.

In this paper we first present a model describing the effect of magnetoelastic coupling on the propagation of rf ultrasonic waves in RbMnF<sub>3</sub>. The predictions of the model are then compared with data obtained in a number of experimental cases. Quantitative as well as qualitative agreement is found for those cases in which

unambiguous theoretical results can be obtained. For other cases, the consequences of the model cannot be directly compared with experiment, owing to our lack of sufficient knowledge concerning the orientation of the sublattice magnetization.

Cole and Ince<sup>3</sup> have given an account of the static equilibrium theory and the antiferromagnetic resonance (AFMR) modes of RbMnF<sub>3</sub> at 4.2 K. Several of their results will be used in the present study. Measurement of the shift in the AFMR frequency on application of a static uniaxial stress enabled Eastman<sup>4</sup> to obtain the values of the two independent magnetoelastic coupling constants (MECC)  $b_1$  and  $b_2$ . Quantitative comparison of our results to his will be made.

In Sec. II the theory of rf ultrasonic propagation in RbMnF<sub>3</sub> is outlined. Those experimental details which are different from those in I are discussed in Sec. III. Section IV is devoted to the presentation of the experimental data and comparison with theory. A brief summary is given in Sec. V.

### II. THEORY

Coupled magnetic and elastic modes in antiferromagnetic insulators have been the subject of several recent theoretical studies.<sup>5-11</sup> These studies have dealt

<sup>3</sup> P. H. Cole and W. J. Ince, Phys. Rev. **150**, 377 (1966).

<sup>4</sup> D. E. Eastman, Phys. Rev. **156**, 645 (1967).

<sup>5</sup> S. V. Peletminskii, Zh. Eksperim. i Teor. Fiz. **37**, 452 (1959) [English transl.: Soviet Phys.—JETP **37**, 321 (1960)].

<sup>6</sup> A. I. Akhiezer, V. G. Bar'yakhtar, and M. L. Kaganov, Usp. Fiz. Nauk **71**, 533 (1960) [English transl.: Soviet Phys.—Usp. **3**, 567 (1961)].

<sup>7</sup> A. I. Mitsek, Fiz. Metal. i Metalloved. **16**, 168 (1963).

<sup>8</sup> M. A. Savchenko, Fiz. Tverd. Tela **6**, 864 (1964) [English transl.: Soviet Phys.—Solid State **6**, 666 (1964)].

<sup>9</sup> V. G. Bar'yakhtar, M. A. Savchenko, and V. V. Tarasenko, Zh. Eksperim. i Teor. Fiz. **49**, 944 (1965) [English transl.: Soviet Phys.—JETP **22**, 657 (1966)].

<sup>10</sup> V. G. Bar'yakhtar and V. V. Gann, Fiz. Tverd. Tela **9**, 2052 (1967) [English transl.: Soviet Phys.—Solid State **9**, 1611 (1968)].

<sup>11</sup> V. V. Gann, Fiz. Tverd. Tela **9**, 3467 (1967) [English transl.: Soviet Phys.—Solid State **9**, 2734 (1968)].

\* Research sponsored in part by the National Science Foundation under Grant No. GP-7931 and the Air Force Office of Scientific Research under Grant No. 68-1412.

† National Science Foundation Graduate Fellow during most of the course of this research. Present address: Laboratory of Atomic and Solid State Physics, Cornell University, Ithaca, N. Y.

<sup>1</sup> R. L. Melcher and D. I. Bolef, Phys. Rev. **178**, 864 (1969).

<sup>2</sup> R. L. Melcher, D. I. Bolef, and R. W. H. Stevenson, Solid State Commun. **5**, 735 (1967).

primarily with uniaxial magnetic systems and have assumed elastic isotropy; as such they are difficult to apply directly to the case of cubic RbMnF<sub>3</sub>, which in many respects is quite different from a uniaxial system. For this reason we present here a detailed calculation applicable specifically to RbMnF<sub>3</sub>. In Sec. II A a brief review of the static and AFMR results is presented. In Sec. II B the effective elastic constants  $C_{ij}^*$  for several types of elastic modes are derived using linear magnetoelastic theory.

### A. Review of Equilibrium and AFMR Theory

Assuming (a) a single-domain sample describable in terms of a two-sublattice molecular-field model and (b) that the equilibrium orientation of each of the sublattice magnetization vectors  $\mathbf{M}_i^0$  ( $i=1, 2$ ) lies in the  $(1\bar{1}0)$  plane, the magnetic free energy of the system can be written in terms of the angle  $\theta$  between the  $[001]$  axis and the vector  $\frac{1}{2}(\mathbf{M}_1^0 - \mathbf{M}_2^0) = \mathbf{M}$  in the  $(1\bar{1}0)$  plane, the angle  $t$  between  $\mathbf{M}$  and  $\mathbf{M}_1^0$ , and the angle  $\psi$  between  $[001]$  and  $\mathbf{H}_0$ , also in the  $(1\bar{1}0)$  plane. This energy expression is then minimized with respect to  $t$  and  $\theta$ , respectively. The result,<sup>3</sup> expressing  $\theta$  in a transcendental equation as a function of  $H_0$  and  $\psi$ , shows that  $\theta$  is strongly dependent upon both  $H_0$  and  $\psi$  for values of  $H_0$  of the order of  $H_c \sim (2H_E H_A)^{1/2}$ . Here  $H_E \approx 8.9 \times 10^5$  Oe and  $H_A \approx 4$  Oe are the respective exchange and anisotropy fields in RbMnF<sub>3</sub>.<sup>12</sup> Thus  $H_c$  is the order of a few kOe.

The AFMR modes in RbMnF<sub>3</sub> were calculated by Cole and Ince<sup>3</sup> by considering the torques exerted on each component of sublattice magnetization as a result of the various magnetic interactions. The agreement with experimentally obtained AFMR spectra was found to be excellent for the case of  $\mathbf{H}_0 \parallel [001]$  although some aspects of the theory were not verified for cases in which  $\mathbf{H}_0$  was aligned along the  $[110]$  or  $[111]$  directions. These minor discrepancies were attributed to part of the sample having a different orientation than the main part, incoherent rotation of the magnetization vectors from positions of local-energy minima to positions of absolute-energy minima, or the overlap of stronger resonances obscuring weaker resonances. The effect of antiferromagnetic domains on the AFMR spectra in RbMnF<sub>3</sub> has also been recently studied.<sup>13</sup>

The approach taken in this paper to the coupling of magnetic and elastic modes is similar to that taken in calculating the AFMR modes. The difference is that we include explicitly the elastic degrees of freedom and magnetoelastic coupling and consider solutions only in the low-frequency limit.

### B. Magnetoelastic Coupling in RbMnF<sub>3</sub>

In this section conventional small-strain magnetoelastic (ME) theory will be applied to the case of a cubic

<sup>12</sup> D. T. Teaney, M. J. Freiser, and R. W. H. Stevenson, Phys. Rev. Letters **9**, 212 (1962).

<sup>13</sup> W. J. Ince and A. Platzker, Phys. Rev. **175**, 650 (1968).

antiferromagnet in which the sublattice magnetization orientation is determined by the magnitude and orientation of an applied magnetic field. Attention will be focused on solutions for frequencies much lower than the AFMR modes and also much lower than the Mn<sup>55</sup> nuclear Larmor frequency ( $\nu \approx 680$  MHz at 4.2 K).<sup>14</sup> The latter condition enables us to exclude effects arising from the nuclear hyperfine term in the free energy, since at these low frequencies the nuclei remain parallel to and exert no torque on the electronic magnetization. The approximations involved in the low-frequency approximation should be valid at all temperatures except in the immediate vicinity of the Néel temperature, i.e.,  $T_N - T \lesssim 2$  K. At the low frequencies under consideration (i.e., long wavelengths) the effect of spacial nonuniformities in the magnetization is negligible and is ignored. Note, however, that at frequencies approaching the AFMR modes (not considered here) such effects become quite important.

The free-energy density for the coupled ME system of cubic symmetry is written

$$E = E_{\text{EX}} + E_Z + E_A + E_E + E_{\text{ME}}. \quad (1)$$

The exchange ( $E_{\text{EX}}$ ), Zeeman ( $E_Z$ ), anisotropy ( $E_A$ ), elastic ( $E_E$ ), and magnetoelastic ( $E_{\text{ME}}$ ) free-energy terms have, respectively, the forms

$$E_{\text{EX}} = -\lambda \mathbf{M}_1 \cdot \mathbf{M}_2, \quad (2)$$

$$E_Z = -\mathbf{H}_0 \cdot (\mathbf{M}_1 + \mathbf{M}_2), \quad (3)$$

$$E_A = -\frac{K}{M_0^4} \sum_{i=1,2} (M_{ix}^2 M_{iy}^2 + \text{c.p.}), \quad (4)$$

$$E_E = \frac{1}{2} C_{11} \sum_{j=x,y,z} e_{jj}^2 + \frac{1}{2} C_{44} (e_{xy}^2 + \text{c.p.}) + C_{12} (e_{xx} e_{yy} + \text{c.p.}) \quad (5)$$

$$E_{\text{ME}} = \frac{B_1}{M_0^2} \sum_{\substack{i=1,2 \\ j=x,y,z}} M_{ij}^2 e_{jj} + \frac{B_3}{M_0^2} \sum_{j=x,y,z} M_{1j} M_{2j} e_{jj} + \frac{B_2}{M_0^2} \sum_{i=1,2} (M_{ix} M_{iy} e_{xy} + \text{c.p.}) + \frac{B_4}{M_0^2} [(M_{1x} M_{2y} + M_{1y} M_{2x}) e_{xy} + \text{c.p.}]. \quad (6)$$

In these expressions c.p. denotes cyclic permutation of  $x, y, z$ ;  $M_{ij}$  is the  $j$ th component ( $j=x, y, z$ ) of the  $i$ th sublattice magnetization ( $i=1, 2$ );  $M_0 = |\mathbf{M}_1| = |\mathbf{M}_2|$ ;  $\mathbf{H}_0$  is the applied dc field,  $C_{11}$ ,  $C_{12}$ , and  $C_{44}$  are the adiabatic elastic constants, and  $B_i$  ( $i=1-4$ ) are the magnetoelastic constants. The strains  $e_{ij}$  are defined in terms of the elastic displacements  $u_i$  ( $\mathbf{r}, t$ ):

$$e_{ij} = (1 - \frac{1}{2} \delta_{ij}) \left( \frac{\partial u_i}{\partial x_j} + \frac{\partial u_j}{\partial x_i} \right). \quad (7)$$

<sup>14</sup> A. J. Heeger and D. T. Teaney, J. Appl. Phys. **35**, 846 (1964).

The exchange constant  $\lambda$  and anisotropy constant  $K$  are related to their respective effective fields by

$$\begin{aligned} H_E &= -\lambda M_0, \\ H_A &= \frac{4}{3}K/M_0. \end{aligned} \quad (8)$$

In Eq. (6) the magnetoelastic coupling arising from crystalline field effects (single ion) and magnetic dipolar forces (two ions) are included. The volume magnetostriction (strain dependence of the exchange interaction) is not included since in the linear approximation used below it contributes only to higher-order terms in the equations of motion.

Denoting the equilibrium orientation of the two sublattices with respect to the crystal coordinate system by the angles  $(\theta_1, \varphi_1)$  and  $(\theta_2, \varphi_2)$ , where  $\theta_1$  and  $\theta_2$  are measured with respect to  $[001]$  and  $\varphi_1$  and  $\varphi_2$  are measured with respect to  $[100]$  in the  $(001)$  plane, the respective free-energy terms are written as shown in Appendix A.

The equations of motion for the "1" magnetic sublattice have the form

$$\frac{dM_{1i}}{dt} = \gamma(\mathbf{M}_1 \times \mathbf{H}_1^{(e)})_i; \quad i = x, y, \quad (9a)$$

$$\frac{dM_{1z}}{dt} = 0; \quad M_{1z} = M_0. \quad (9b)$$

Equation (9b) is a consequence of the linear approximation.<sup>15</sup>  $\gamma$  is the electronic gyromagnetic ratio ( $\gamma < 0$ ). The effective field  $\mathbf{H}_1^{(e)}$  acting on the "1" sublattice is given by

$$\mathbf{H}_1^{(e)} = -\frac{\partial E}{\partial \mathbf{M}_1}. \quad (10)$$

The equations corresponding to the "2" sublattice are obtained through the substitution  $1 \rightarrow 2$  in Eqs. (9) and (10).

The equations of motion for the elastic displacements

have the form

$$\begin{aligned} \rho \frac{\partial^2 u_x}{\partial t^2} &= \frac{\partial^2 E}{\partial x \partial e_{xx}} + \frac{\partial^2 E}{\partial y \partial e_{xy}} + \frac{\partial^2 E}{\partial z \partial e_{xz}} \\ &+ \mathbf{M}_1 \cdot \frac{\partial \mathbf{H}_1^{(e)}}{\partial x} + \mathbf{M}_2 \cdot \frac{\partial \mathbf{H}_2^{(e)}}{\partial x}, \end{aligned} \quad (11)$$

with c.p. of  $x, y, z$  to obtain the equations for  $u_y$  and  $u_z$ . The first three terms on the right-hand side of Eq. (11) are the forces resulting both from elastic and from magnetoelastic stresses and the last two terms represent magnetic body forces. In Eqs. (9) and (11) we have omitted any dissipative terms.

Linearizing the Eqs. (9a) and (11) with respect to the variables  $M_{ij}$  and  $u_k$  and assuming harmonic behavior of the form

$$M_{ij} \sim u_k \sim e^{i(\omega t - \mathbf{k} \cdot \mathbf{r})}, \quad (12)$$

with  $i = 1, 2, j = x, y$ , and  $k = x, y, z$  we obtain a set of seven simultaneous, linear, homogeneous, algebraic equations in the four magnetic and three elastic variables.

Up to this point our treatment has been quite general in that arbitrary orientations of the dc field  $\mathbf{H}_0$  and the equilibrium sublattice vectors  $\mathbf{M}_1^0$  and  $\mathbf{M}_2^0$  have been allowed. A considerable simplification results if the field  $\mathbf{H}_0$  is restricted to lie in the  $(1\bar{1}0)$  crystallographic plane and  $\mathbf{M}_1^0$  and  $\mathbf{M}_2^0$  are assumed to lie in this plane. These are the same restrictions used in deriving the equilibrium orientation results.<sup>3</sup> Thus, setting  $\varphi_1 = \varphi_2 = \frac{1}{4}\pi$  and defining  $\theta$  to be the angle that  $\mathbf{M} = \frac{1}{2}(\mathbf{M}_1^0 - \mathbf{M}_2^0)$  makes with respect to  $[001]$  we have  $\theta_1 = \theta - t$  and  $\theta_2 = \theta + t + \pi$ , where  $t$  is the tilt angle of  $\mathbf{M}_1^0$  with respect to  $\mathbf{M}$ . The angle which  $\mathbf{H}_0$  makes with  $[001]$  is denoted by  $\psi$  and the angle  $\varphi$  is defined by  $\varphi = \theta - \psi$ .

With this notation the seven simultaneous equations take the form<sup>16</sup>

$$\begin{pmatrix} \Gamma_{xx} & \Gamma_{xy} & \Gamma_{xz} & \frac{i}{M_0}(t_{21} + S_x^-) & -\frac{i}{M_0}t_{11} & -\frac{i}{M_0}(t_{21} + S_x^+) & \frac{i}{M_0}t_{11} \\ \Gamma_{yx} & \Gamma_{yy} & \Gamma_{yz} & \frac{i}{M_0}(t_{22} + S_y^-) & -\frac{i}{M_0}t_{12} & -\frac{i}{M_0}(t_{22} + S_y^+) & \frac{i}{M_0}t_{12} \\ \Gamma_{zx} & \Gamma_{zy} & \Gamma_{zz} & \frac{i}{M_0}(t_{23} + S_z^-) & -\frac{i}{M_0}t_{13} & -\frac{i}{M_0}(t_{23} + S_z^+) & \frac{i}{M_0}t_{13} \\ i\gamma t_{11} & i\gamma t_{12} & i\gamma t_{13} & a & b & 0 & d \\ i\gamma t_{21} & i\gamma t_{22} & i\gamma t_{23} & c & a & -e & 0 \\ i\gamma t_{11} & i\gamma t_{12} & i\gamma t_{13} & 0 & -d & a & f \\ i\gamma t_{21} & i\gamma t_{22} & i\gamma t_{23} & e & 0 & g & a \end{pmatrix} \begin{pmatrix} u_x \\ u_y \\ u_z \\ M_{1x} \\ M_{1y} \\ M_{2x} \\ M_{2y} \end{pmatrix} = 0. \quad (13)$$

<sup>15</sup> Note that in Eqs. (9) and (10) and henceforth in this paper, unless otherwise specified, the magnetic variables are expressed in the equilibrium coordinate systems defined in Appendix A.

<sup>16</sup> R. L. Melcher, Ph.D. thesis, Washington University, St. Louis, Mo., 1968 (unpublished).

TABLE I. Solutions for several elastic modes in the weak-coupling limit with  $\mathbf{H}_0$  in the  $(1\bar{1}0)$  plane.

Elastic mode		Solution <sup>a</sup>
1	$\mathbf{k}_{\text{long}} \parallel [001]$	$C_{11}^* = C_{11} - 4b_1 \cos^2\theta + 4 \frac{\gamma\omega_E b_1^2 \sin^2 2\theta}{M_0 \omega_+^2} \left\{ 1 - \frac{3K}{b_1} (1 - \frac{3}{2} \sin^2\theta) - \frac{H_0}{4H_E} \frac{H_0 M_0 \sin 2\varphi}{b_1 \sin 2\theta} \right\}$
2	$\mathbf{k}_{\text{long}} \parallel [100]$	$C_{11}^* = C_{11} - 2b_1 \sin^2\theta + 4 \left( \frac{\gamma\omega_E}{M_0} \right) b_1^2 \left\{ \frac{\sin^2\theta}{\omega_-^2} + \frac{1 \sin^2 2\theta}{4 \omega_+^2} \left[ 1 + \frac{6K}{b_1} (1 - \frac{3}{2} \sin^2\theta) + \frac{H_0}{2H_E} \frac{M_0 H_0 \sin 2\varphi}{b_1 \sin 2\theta} \right] \right\}$
	(i) $\mathbf{k}_{\text{trans}} \parallel [001]$	$C_{44}^* = C_{44} + 4 \frac{\gamma\omega_E b_2^2 \cos^2\theta}{M_0 \omega_-^2}$
	(ii) $\mathbf{k}_{\text{trans}} \parallel [001]$	$C_{44}^* = C_{44} + 4 \frac{\gamma\omega_E b_2^2 \cos^2 2\theta}{M_0 \omega_+^2}$
4	$\mathbf{k}_{\text{long}} \parallel [110]$	$C_L^* = C_L - 2(b_1 + b_2) \sin^2\theta + \frac{\gamma\omega_E (b_1 + b_2)^2}{M_0 \omega_+^2} \sin^2 2\theta \left\{ 1 + \frac{6K}{b_1 + b_2} (1 - \frac{3}{2} \sin^2\theta) + \frac{H_0}{2H_E} \frac{M_0 H_0 \sin 2\varphi}{(b_1 + b_2) \sin 2\theta} \right\}$
5	$\mathbf{k}_{\text{long}} \parallel [\bar{1}10]$	$C_L^* = C_L - 2(b_1 - b_2) \sin^2\theta + \frac{\gamma\omega_E (b_1 - b_2)^2}{M_0 \omega_+^2} \sin^2 2\theta \left\{ 1 + \frac{6K}{b_1 - b_2} (1 - \frac{3}{2} \sin^2\theta) + \frac{H_0}{2H_E} \frac{M_0 H_0 \sin 2\varphi}{(b_1 - b_2) \sin 2\theta} \right\}$
6 <sup>c</sup>	$\mathbf{k}_{\text{long}} \parallel [101]$	$C_L^* \simeq C_L + \frac{2\gamma\omega_E}{M_0} \left[ \frac{1}{\omega_-^2} \left( \frac{b_1 \sin\theta}{\sqrt{2}} + b_2 \cos\theta \right)^2 + \frac{1}{\omega_+^2} \left( \frac{b_1 \sin 2\theta}{2\sqrt{2}} - b_2 \cos 2\theta \right)^2 \right]$
7 <sup>b</sup>	$\mathbf{k}_{\text{long}} \parallel [\bar{1}01]$	$C_L^* \simeq C_L + 2 \frac{\gamma\omega_E}{M_0} \left[ \frac{1}{\omega_-^2} \left( \frac{b_1 \sin\theta}{\sqrt{2}} - b_2 \cos\theta \right)^2 + \frac{1}{\omega_+^2} \left( \frac{b_1 \sin 2\theta}{2\sqrt{2}} + b_2 \cos 2\theta \right)^2 \right]$
8	$\mathbf{k}_{\text{trans}} \parallel [110]$ $\mathcal{E} \parallel [001]$	$C_{44}^* = C_{44} + 4 \frac{\gamma\omega_E b_2^2 \cos^2 2\theta}{M_0 \omega_+^2}$
9	$\mathbf{k}_{\text{trans}} \parallel [1\bar{1}0]$ $\mathcal{E} \parallel [001]$	$C_{44}^* = C_{44} + 4 \frac{\gamma\omega_E b_2^2 \cos^2\theta}{M_0 \omega_-^2}$
10	$\mathbf{k}_{\text{trans}} \parallel [110]$ or $[1\bar{1}0]$ $\mathcal{E} \parallel [1\bar{1}0]$ or $[110]$	$C'^* = C' + 4 \frac{\gamma\omega_E b_1^2 \sin^2\theta}{M_0 \omega_-^2}$
11	$\mathbf{k}_{\text{trans}} \parallel [101]$ or $[\bar{1}01]$ $\mathcal{E} \parallel [\bar{1}01]$ or $[101]$	$C'^* = C' + \frac{\gamma\omega_E b_1^2 \sin^2\theta}{M_0 \omega_-^2} \left[ 1 + 9 \frac{\omega_-^2}{\omega_+^2} \cos^2\theta \right]$

<sup>a</sup>  $\omega_{\pm}^2 = 2a_{21}\omega_E + \omega_0^2 (2\sin^2\varphi - 1)$ ,  $\omega_-^2 = -[2a_{12}\omega_E + \omega_0^2 \cos^2\varphi]$ .<sup>b</sup> The magnetic-body force terms have been omitted for simplicity in rows 6 and 7.

The quantities  $\Gamma_{ij}$ ,  $t_{kl}$ ,  $S_m^{\pm}$ , ( $i, j = x, y, z$ ,  $k = 1, 2, l = 1, 2, 3$ , and  $m = x, y, z$ ) and  $a-g$  are all defined in Appendix B.<sup>17</sup> There result only two independent MECC  $b_1$  and  $b_2$  defined by

$$\begin{aligned} b_1 &= B_1 - \frac{1}{2} B_3, \\ b_2 &= B_2 - B_4. \end{aligned} \quad (14)$$

Our primary interest is in the quasielastic solutions to Eqs. (13). The upper left-hand  $3 \times 3$  matrix  $\Gamma_{ij}$  is

<sup>17</sup> Equations (13) can be equivalently derived in the following manner. In the crystal coordinate system write the nine equations of motion corresponding to the six magnetic and three elastic degrees of freedom. Apply the transformation which transforms to the equilibrium coordinate systems to these nine equations and delete the resulting equations for  $M_{1z}$  and  $M_{2z}$  [corresponding to Eq. (9b)]. The result is then exactly Eqs. (13). This approach was taken in Ref. 16 and is quite analogous to that used in Ref. 3 to calculate the AFMR modes.

(with the addition of part of the magnetic-body force terms) the matrix of elastic constants obtained for an elastic medium of cubic symmetry. The lower right-hand  $4 \times 4$  matrix is that used to calculate the AFMR modes (because we are considering the low-frequency limit, the terms involving the hyperfine interaction with the  $\text{Mn}^{55}$  nuclear spins have been omitted). The coupling terms in  $t_{kl}$  correspond to magnetoelastic stresses and torques, while those in  $S_m^{\pm}$  are derived from the magnetic-body forces.

Solutions exist for Eqs. (13) only if the  $7 \times 7$  determinant of coefficients is zero. The general secular equation is quite complex and we restrict ourselves to propagation along the  $[100]$  and  $[110]$  (or equivalent) axes. In addition, the solutions will be obtained in the weak coupling approximation; the effect of magnetoelastic coupling is considered to be a small perturbation

TABLE II. Solutions for  $\mathbf{H}_0 \parallel [001]$ .<sup>a</sup>

Elastic mode		Solutions
1	$\mathbf{k}_{\text{long}} \parallel [001]$	$C_{11}^* = C_{11} - \frac{4}{3} b_1 + \frac{20}{9} \frac{H_0^2}{H_E H_A} - \frac{4}{3} \frac{b_1^2}{K}$ ; $H_0 \leq (\frac{2}{3} H_E H_A)^{1/2}$ $C_{11}^* = C_{11}$ ; $H_0 \geq (\frac{2}{3} H_E H_A)^{1/2}$
2	$\mathbf{k}_{\text{long}} \parallel [100]$	$C_{11}^* = C_{11} - \frac{4}{3} b_1 - \frac{10}{9} \frac{H_0^2}{H_E H_A} - \frac{4}{3} \frac{b_1^2}{K}$ ; $H_0 \leq (\frac{2}{3} H_E H_A)^{1/2}$ $C_{11}^* = C_{11} - 2b_1 - \frac{b_1^2}{K}$ ; $H_0 \geq (\frac{2}{3} H_E H_A)^{1/2}$
3	$\mathbf{k}_{\text{trans}} \parallel [001]$	(i) $C_{44}^* = C_{44} - \frac{1}{2} \frac{b_2^2 [1 - \frac{2}{3} (H_0^2 / H_E H_A)]}{K [1 + \frac{1}{3} (H_0^2 / H_E H_A)]}$ ; $H_0 \leq (\frac{2}{3} H_E H_A)^{1/2}$ $C_{44}^* = C_{44}$ ; $H_0 \geq (\frac{2}{3} H_E H_A)^{1/2}$
		(ii) $C_{44}^* = C_{44} - \frac{1}{6} \frac{b_2^2 \left( 1 + \frac{8}{3} \frac{H_0^2}{H_E H_A} + \frac{16}{9} \frac{H_0^4}{H_E^2 H_A^2} \right)}{K} \bigg/ \left( 1 - \frac{1}{3} \frac{H_0^2}{H_E H_A} - \frac{2}{9} \frac{H_0^4}{H_E^2 H_A^2} \right)$ ; $H_0 \leq (\frac{2}{3} H_E H_A)^{1/2}$ $C_{44}^* = C_{44} + 2 \frac{b_2^2}{K} \bigg/ \left( 1 - \frac{2}{3} \frac{H_0^2}{H_E H_A} \right)$ ; $H_0 \geq (\frac{2}{3} H_E H_A)^{1/2}$
4	$\mathbf{k}_{\text{long}} \parallel [110]$	$C_L^* = C_L - \frac{4}{3} (b_1 + b_2) - \frac{10}{9} (b_1 + b_2) \frac{H_0^2}{H_E H_A} - \frac{1}{3} \frac{(b_1 + b_2)^2}{K}$ ; $H_0 \leq (\frac{2}{3} H_E H_A)^{1/2}$ $C_L^* = C_L - 2(b_1 + b_2)$ ; $H_0 \geq (\frac{2}{3} H_E H_A)^{1/2}$
5	$\mathbf{k}_{\text{long}} \parallel [1\bar{1}0]$	$C_L^* = C_L - \frac{4}{3} (b_1 - b_2) - \frac{10}{9} (b_1 - b_2) \frac{H_0^2}{H_E H_A} - \frac{1}{3} \frac{(b_1 - b_2)^2}{K}$ ; $H_0 \leq (\frac{2}{3} H_E H_A)^{1/2}$ $C_L^* = C_L - 2(b_1 - b_2)$ ; $H_0 \geq (\frac{2}{3} H_E H_A)^{1/2}$
6	$\mathbf{k}_{\text{long}} \parallel [101]$	$C_L^* \simeq C_L - \frac{1}{3K} (b_1^2 + b_2^2 + b_1 b_2)$ ; $H_0 = 0$ $C_L^* \simeq C_L - \frac{1}{4K} \left[ b_1^2 - 4b_2^2 \bigg/ \left( 1 - \frac{2}{3} \frac{H_0^2}{H_E H_A} \right) \right]$ ; $H_0 \geq (\frac{2}{3} H_E H_A)^{1/2}$
7	$\mathbf{k}_{\text{long}} \parallel [\bar{1}01]$	$C_L^* \simeq C_L - \frac{1}{3K} (b_1^2 + b_2^2 - b_1 b_2)$ ; $H_0 = 0$ $C_L^* \simeq C_L - \frac{1}{4K} \left[ b_1^2 - 4b_2^2 \bigg/ \left( 1 - \frac{2}{3} \frac{H_0^2}{H_E H_A} \right) \right]$ ; $H_0 \geq (\frac{2}{3} H_E H_A)^{1/2}$
8	$\mathbf{k}_{\text{trans}} \parallel [110]$ $\mathcal{E} \parallel [001]$	$C_{44}^* = C_{44} - \frac{1}{6} \frac{b_2^2 [1 + (8/3)(H_0^2 / H_E H_A) + (16/9)(H_0^4 / H_E^2 H_A^2)]}{K [1 - \frac{1}{3} (H_0^2 / H_E H_A) - (2/9)(H_0^4 / H_E^2 H_A^2)]}$ ; $H_0 \leq (\frac{2}{3} H_E H_A)^{1/2}$ $C_{44}^* = C_{44} + 2 \frac{b_2^2}{K} \bigg/ \left( 1 - \frac{2}{3} \frac{H_0^2}{H_E H_A} \right)$ ; $H_0 \geq (\frac{2}{3} H_E H_A)^{1/2}$
9	$\mathbf{k}_{\text{trans}} \parallel [1\bar{1}0]$ $\mathcal{E} \parallel [001]$	$C_{44}^* = C_{44} - \frac{1}{2} \frac{b_2^2 (1 - \frac{2}{3} H_0^2 / H_E H_A)}{K (1 + \frac{1}{3} H_0^2 / H_E H_A)}$ ; $H_0 \leq (\frac{2}{3} H_E H_A)^{1/2}$ $C_{44}^* = C_{44}$ ; $H_0 \geq (\frac{2}{3} H_E H_A)^{1/2}$
10	$\mathbf{k}_{\text{trans}} \parallel [110]$ or $[1\bar{1}0]$ $\mathcal{E} \parallel [1\bar{1}0]$ or $[110]$	$C'^* = C' - \frac{b_1^2}{K}$ ; all $H_0$ $C'^* = C' - \frac{b_1^2}{K}$ ; $H_0 \leq (\frac{2}{3} H_E H_A)^{1/2}$
11	$\mathbf{k}_{\text{trans}} \parallel [101]$ or $[\bar{1}01]$ $\mathcal{E} \parallel [\bar{1}01]$ or $[101]$	$C'^* = C' - \frac{b_1^2}{4K}$ ; $H_0 \geq (\frac{2}{3} H_E H_A)^{1/2}$

<sup>a</sup> The initial condition that  $\mathbf{M}_1 \parallel [111]$  for  $H_0 = 0$  is assumed for each case.<sup>b</sup> The magnetic-body force terms have been omitted for simplicity in rows 6 and 7.

TABLE III. Solutions for  $\mathbf{H}_0 \parallel [111]$ .<sup>a,b</sup>

	Elastic mode	Solution
1	$\mathbf{k}_{\text{long}} \parallel [001]$	$C_{11}^* = C_{11} - \frac{4}{3} b_1 - \frac{4}{3} \frac{b_1^2}{K}; H_0 = 0$ $C_{11}^* \rightarrow C_{11} - (8/3)b_1; H_0 \gg (2H_E H_A)^{1/2}$
2	$\mathbf{k}_{\text{long}} \parallel [100]$	$C_{11}^* = C_{11} - \frac{4}{3} b_1 - \frac{4}{3} \frac{b_1^2}{K}; H_0 = 0$ $C_{11}^* \rightarrow 0; H_0 \gg (2H_E H_A)^{1/2}$
3	$\mathbf{k}_{\text{trans}} \parallel [001]$	$C_{44}^* = C_{44} - \frac{1}{2} \frac{b_2^2}{K}; H_0 = 0$ (i) $C_{44}^* \rightarrow 0; H_0 \gg (2H_E H_A)^{1/2}$ $C_{44}^* = C_{44} - \frac{1}{6} \frac{b_2^2}{K}; H_0 = 0$ (ii) $C_{44}^* \rightarrow C_{44}; H_0 \gg (2H_E H_A)^{1/2}$
4	$\mathbf{k}_{\text{long}} \parallel [110]$	$C_L^* = C_L - \frac{4}{3} (b_1 + b_2) - \frac{1}{3} \frac{(b_1 + b_2)^2}{K}; H_0 = 0$ $C_L^* \rightarrow C_L - \frac{2}{3} (b_1 + b_2); H_0 \gg (2H_E H_A)^{1/2}$
5	$\mathbf{k}_{\text{long}} \parallel [1\bar{1}0]$	$C_L^* = C_L - \frac{4}{3} (b_1 - b_2) - \frac{1}{3} \frac{(b_1 - b_2)^2}{K}; H_0 = 0$ $C_L^* \rightarrow C_L - \frac{2}{3} (b_1 - b_2); H_0 \gg (2H_E H_A)^{1/2}$
6 <sup>c</sup>	$\mathbf{k}_{\text{long}} \parallel [101]$	$C_L^* \simeq C_L - \frac{1}{3K} (b_1^2 + b_2^2 - b_1 b_2); H_0 = 0$ $C_L^* \rightarrow 0; H_0 \gg (2H_E H_A)^{1/2}$
7 <sup>c</sup>	$\mathbf{k}_{\text{long}} \parallel [\bar{1}01]$	$C_L^* \simeq C_L - \frac{1}{3K} (b_1^2 + b_2^2 - b_1 b_2); H_0 = 0$ $C_L^* \rightarrow 0; H_0 \gg (2H_E H_A)^{1/2}$
8	$\mathbf{k}_{\text{trans}} \parallel [110]$	$C_{44}^* = C_{44} - \frac{1}{6} \frac{b_2^2}{K}; H_0 = 0$
	$\mathcal{E} \parallel [001]$	$C_{44}^* \rightarrow C_{44}; H_0 \gg (2H_E H_A)^{1/2}$
9	$\mathbf{k}_{\text{trans}} \parallel [1\bar{1}0]$	$C_{44}^* = C_{44} - \frac{1}{2} \frac{b_2^2}{K}; H_0 = 0$
	$\mathcal{E} \parallel [001]$	$C_{44}^* \rightarrow 0; H_0 \gg (2H_E H_A)^{1/2}$
10	$\mathbf{k}_{\text{trans}} \parallel [110] \text{ or } [1\bar{1}0]$	$C'^* = C' - \frac{b_1^2}{K}; H_0 = 0$
	$\mathcal{E} \parallel [1\bar{1}0] \text{ or } [110]$	$C'^* \rightarrow 0; H_0 \gg (2H_E H_A)^{1/2}$
	$\mathbf{k}_{\text{trans}} \parallel [101] \text{ or } [\bar{1}01]$	$C'^* = C' - \frac{b_1^2}{K}; H_0 = 0$
11	$\mathcal{E} \parallel [\bar{1}01] \text{ or } [101]$	$C'^* \rightarrow 0; H_0 \gg (2H_E H_A)^{1/2}$

<sup>a</sup>  $C_{ij}^* \rightarrow 0, H_0 \gg (2H_E H_A)^{1/2}$  means that the measured elastic constant is predicted to decrease monotonically with increasing  $H_0$  for large  $H_0$ .  
<sup>b</sup> For  $H_0 = 0, \mathbf{M}_i \parallel [111]$  and for  $H_0 \neq 0, \mathbf{M}$  is assumed to remain in the  $(1\bar{1}0)$  plane.  
<sup>c</sup> The magnetic-body force terms have been omitted for simplicity in rows 6 and 7.

on the quasielastic modes and it is assumed that no significant mixing of the elastic modes occurs.

The solutions to Eqs. (13) in this approximation for longitudinal and transverse modes propagating along cubic axes and face diagonals are given in Table I for

$\mathbf{H}_0$  in the  $(1\bar{1}0)$  plane. The solutions take the form of an effective elastic constant  $C_{ij}^*$ :

$$\rho v^2 = C_{ij}^* = C_{ij} + f_{ij}(b_k, \mathbf{H}_0, \theta, K, H_E, M_0), \quad (15)$$

where  $v = \omega/k$  is the ultrasonic phase velocity and  $\rho$  is

the density. The terms linear in the MECC  $b_1$  and  $b_2$ , which arise from the magnetic-body forces, are seen to contribute as expected only to the quasilongitudinal elastic modes. The results of the static equilibrium theory<sup>3</sup> must be used to express  $\theta$  as a function of  $\mathbf{H}_0$ . For a given orientation of  $\mathbf{H}_0$ , the term  $f_{ij}$  is thus dependent only on the magnitude of  $\mathbf{H}_0$  and on the temperature-dependent constants  $b_k(T)$ ,  $M_0(T)$ ,  $K(T)$ , and  $H_E$ , characteristic of the material. The lack of frequency dependence of  $f_{ij}$  is a consequence of our low-frequency approximation.

We now discuss, as examples, three experimental situations, and defer discussion of the others until Sec. IV. In Table II are shown the theoretical results for  $\mathbf{H}_0 \parallel [001]$  and in Table III are shown the results for  $\mathbf{H}_0 \parallel [111]$ . In Table III, because of the complexity of the equations for arbitrary magnitudes of  $\mathbf{H}_0$ , only the limiting cases for  $H_0=0$  and  $H_0 \gg (2H_E H_A)^{1/2}$  are presented. These indicate simply whether the measured elastic constant is expected to increase or decrease with increasing  $H_0$ .

(i) Consider longitudinal waves propagating along the  $[001]$  axis with  $\mathbf{H}_0 \parallel \mathbf{k} \parallel [001]$ . According to the equilibrium theory,<sup>3</sup> if we assume that  $\mathbf{M}_1^0 \parallel [111]$  for  $H_0=0$ , then for  $H_0 \neq 0$  the vector  $\mathbf{M}$  will rotate in the  $(1\bar{1}0)$  plane; the angle  $\theta = \angle(\mathbf{M}, [001])$  is related to  $H_0$  by

$$\frac{4}{3} \frac{H_0^2}{H_E H_A} = 1 + 3 \cos 2\theta, \quad H_0 \leq (\frac{3}{2} H_E H_A)^{1/2}$$

$$\theta = \frac{1}{2}\pi, \quad H_0 \geq (\frac{3}{2} H_E H_A)^{1/2}. \quad (16)$$

Because of the symmetry of the  $[001]$  axis with respect to the four equivalent  $[111]$  axes (i.e., the four possible antiferromagnetic domains) and to the  $(1\bar{1}0)$  and  $(110)$  planes, it is immaterial whether the magnetization lies in the  $(1\bar{1}0)$  or the  $(110)$  plane or is distributed in domains between these two planes. The results of the magnetoelastic theory are independent of the initial conditions placed on  $\mathbf{M}_1^0$  and  $\mathbf{M}_2^0$ . The results for this case are given by row 1 of Table II. As we demonstrate in Sec. IV, the experimental data are in excellent agreement with theory in this case.

(ii) We now consider the case of  $\mathbf{H}_0 \parallel [111]$ . The equilibrium theory is not easily expressed analytically for arbitrary  $H_0$  and we restrict ourselves to the limiting cases of  $H_0=0$ , and  $H_0 \gg (2H_E H_A)^{1/2}$ . For  $H_0=0$ ,  $\mathbf{M}_1^0 \parallel [111]$ ; for  $H_0 \gg (2H_E H_A)^{1/2}$ ,  $\mathbf{M}$  lies in the  $(1\bar{1}0)$  plane perpendicular to  $\mathbf{H}_0$ . The results of the calculation for longitudinal waves propagating along  $[001]$  and  $[100]$  are given in rows 1 and 2 of Table III. Experimentally, these two cases are identical. The theory gives different results because the  $(1\bar{1}0)$  plane is not symmetrical with respect to the  $[001]$  and  $[100]$  axes and the assumption of the equilibrium theory is that  $\mathbf{M}$  lies always in the  $(1\bar{1}0)$  plane. Experimentally, at 4.2°K all

of the measured elastic constants show a decrease on increasing  $H_0$  when  $\mathbf{H}_0 \parallel [111]$ .

(iii) When  $\mathbf{H}_0 \parallel [110]$  the equilibrium results are even more difficult to express analytically since  $\mathbf{M}$  is known to rotate or flip out of the  $(1\bar{1}0)$  plane for  $H_0$  between 0 and  $(3H_E H_A)^{1/2}$ .<sup>3</sup> Although we will not be concerned in any detail with this case it is interesting to note that antiferromagnetic domains<sup>13</sup> behave quite differently for this field orientation depending upon whether  $\mathbf{M}$  for a given domain lies initially (i.e., for  $H_0=0$ ) in the  $(1\bar{1}0)$  plane or in the  $(110)$  plane. Apparent discontinuities in the data for  $\mathbf{H}_0 \parallel [110]$  and  $H_0 \approx 1$  kOe are attributed below to such domain effects.

### III. EXPERIMENTAL

The two single-crystal specimens of RbMnF<sub>3</sub> (S3A and S3B) used in the present study and their preparation were described in I.<sup>1</sup>

The cw transmission technique described in I was used to obtain the elastic constant data taken at  $\sim 30$  MHz. The data taken at  $\sim 10$  MHz were obtained through use of the cw  $Q$ -meter technique.<sup>18,19</sup> The data are presented as the relative change in the effective elastic constant  $C_{ij}^*$  as a function of magnetic field—both magnitude and orientation. The relationship between the change in frequency of the  $n$ th mechanical resonance  $\Delta\nu$  and the change in the elastic constant  $\Delta C_{ij} = C_{ij}^* - C_{ij}$  is given by

$$\Delta C_{ij}/C_{ij} = 2(\Delta\nu/\nu_0), \quad (17)$$

where magnetostrictive sample length changes are neglected (see Sec. IV D) and  $\nu_0$  is the mechanical resonance frequency corresponding to the “pure” elastic constant  $C_{ij}$ .

The effective resistance presented to the  $Q$  meter by the composite resonator consisting of the specimen-plus-quartz transducer can be shown to be proportional to the ultrasonic attenuation.<sup>18</sup> The attenuation measurements taken at  $\sim 10$  MHz were obtained with this method and are given in arbitrary units.

### IV. EXPERIMENTAL RESULTS AND DISCUSSION

The presentation of the data is divided into four subsections. Section IV A deals with the dependence of the effective elastic constants on the magnitude of magnetic fields applied along symmetry axes of the crystal at 4.2 K. In Sec. IV B, elastic constant and attenuation measurements are presented as functions of the orientation of the applied field at both 4.2 and 77.4 K. The temperature dependence is discussed in Sec. IV C, and Sec. IV D magnetostrictive effects are discussed.

<sup>18</sup> D. I. Bolef and M. Menes, J. Appl. Phys. **31**, 1010 (1960).

<sup>19</sup> D. I. Bolef and J. de Klerk, Trans. IEEE **UE-10**, 19 (1963).

**A. Magnetic Field Dependence of Elastic Constants at 4.2 K**

In the following we summarize the experimental data and present a comparison with the theory given in Sec. II. The simplification that the magnetic-body force terms are negligible is made throughout. Consideration of the relative magnitudes of  $b_1$ ,  $b_2$ ,  $K$ ,  $H_E$ ,  $H_0$ , and  $M_0$  show that this is a very good approximation.

*1. Longitudinal Waves, k Parallel to Cubic Axis*

In Fig. 1 are presented the data obtained at  $\nu \approx 10.6$  MHz for  $\mathbf{k} \parallel [001]$  with  $\mathbf{H}_0$  aligned along the  $[001]$ ,  $[111]$ , and  $[110]$  axes. When  $\mathbf{k} \parallel [100]$  and  $\mathbf{H}_0 \parallel [100]$ ,  $[001]$ , and  $[101]$ , the data for  $\nu \approx 30.0$  MHz are as shown in Fig. 2.

For both cases in which  $\mathbf{H}_0 \parallel \mathbf{k}$ , theory yields the results shown in row 1 of Table II; the prediction of a discontinuous change in  $C_{11}^*$  by  $\Delta C_{11}^* = -4b_1^2/3K$  at  $H_0 = H_c = (\frac{3}{2}H_E H_A)^{1/2}$  agrees quite well with the data shown on Figs. 1 and 2. Quantitative comparison with theory is made in rows 1 and 2 of Table IV, where the assumption is made that  $H_c$  corresponds to that magnetic field at which  $C_{ij}^*(H_0)$  has a maximum slope. The agreement between rows 1 and 2 of Table IV confirms also the lack of frequency dependence of  $C_{11}^*$  in the frequency range of the present experiments.

When  $\mathbf{H}_0$  is aligned along a different cubic axis at right angles to the propagation direction (Fig. 2) the appropriate expression is given in row 2 of Table II. The comparison with experimental results is given by row 3 of Table IV. The values shown in parenthesis are those obtained using the same value of  $H_c$  as in the above two cases. The quantitative agreement with theory is striking for these three cases. Because of symmetry no domain effects are expected in these cases and none are observed.

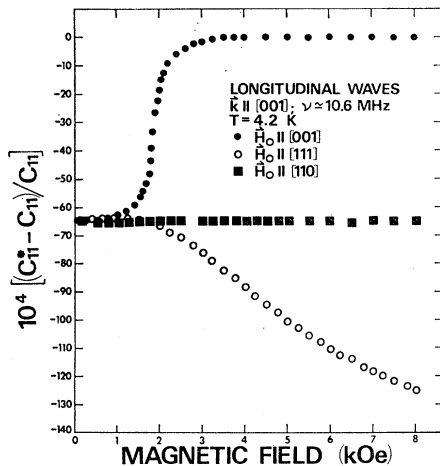


FIG. 1. Relative change in the elastic constant  $C_{11}^*$  versus magnetic field for  $\mathbf{H}_0$  applied along three symmetry directions in the (110) plane;  $T = 4.2$  K.

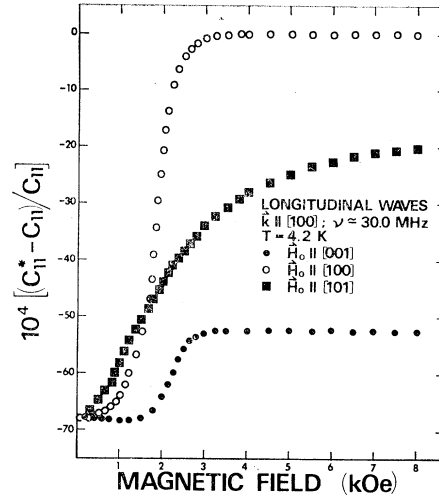


FIG. 2. Relative change in the elastic constant  $C_{11}^*$  versus magnetic field for  $\mathbf{H}_0$  applied along three symmetry directions in the (010) plane;  $T = 4.2$  K.

When the magnetic field is applied along the “easy”  $[111]$  direction the experimental situation is independent of along which equivalent  $[100]$  axis  $\mathbf{k}$  is aligned. However, the theoretical results for  $\mathbf{k} \parallel [001]$  (row 1 Table III) and for  $\mathbf{k} \parallel [100]$  or  $[010]$  (row 2 of Table III) are quite different as discussed in Sec. II. For  $H_0 \gg (2H_E H_A)^{1/2}$  the orientation of  $\mathbf{M}_1^0$  with respect to  $\mathbf{k}$  is different for  $\mathbf{k} \parallel [001]$  than for  $\mathbf{k} \parallel [100]$  or  $[010]$ , thus leading to the discrepancy between rows 1 and 2 of Table III. Experimentally, the data (Fig. 1) show that  $C_{11}^*$  decreases with increasing  $H_0$ .

When  $\mathbf{H}_0 \parallel [110] \perp \mathbf{k} \parallel [001]$ , the measured elastic constant is independent of  $H_0$  (Fig. 1). However, if  $\mathbf{H}_0 \parallel [101]$  and  $\mathbf{k} \parallel [100]$ , then  $C_{11}^*$  increases monotonically with increasing  $H_0$  (Fig. 2).

*2. Transverse Waves, k || [001], e || [110] or [100]*

Rows 3(i) and 3(ii) of Table I show that the degeneracy of the pure elastic mode is lifted by the inclusion of magnetoelastic coupling. However, any small perturbation (i.e., a slight misorientation of the crystalline axes) will also break the symmetry which causes the degeneracy; quantitative measurements are thus difficult to make with this mode. Since the two nondegenerate modes given in row 3 Table I are characterized by the coupling constant  $b_2$ , some qualitative estimate of  $b_2$  can be made. To within the experimental error of  $\pm 0.004\%$ ,  $C_{44}^*$  (not shown here) was found to be independent of  $H_0$  regardless of the orientation of  $\mathbf{H}_0$  with respect to  $\mathbf{k}$ , with the exception of  $\mathbf{H}_0 \parallel [111]$ . In the latter case ( $\mathbf{H}_0 \parallel [111]$ ), a monotonic decrease in  $C_{44}^*$  of magnitude  $\Delta C_{44} = 0.008\%$  was found on increasing  $H_0$  from zero to 8 kOe. The weak magnetic field dependence for the  $C_{44}$  mode indicates that  $b_2 \ll b_1$ .

TABLE IV. Comparison of theory with experiment.<sup>a</sup>

	Elastic mode; field orientation	Frequency (MHz)	H <sub>e</sub> (kOe) (expt)	$\frac{\Delta C_{ij}^*}{C_{ij}}$ (expt)	$\frac{\Delta C_{ij}^*}{C_{ij}}$ (theoret)	$\left(\frac{K^b}{10^3 \frac{\text{ergs}}{\text{cm}^2}}\right)$ (expt)	$\left(\frac{b^c}{10^6 \frac{\text{ergs}}{\text{cm}^2}}\right)$ (expt)
1	<b>k</b> <sub>long</sub>   [001]	10.6	1.85	6.49×10 <sup>-3</sup>	$\frac{4}{3} \frac{b_1^2}{C_{11}K}$	0.586	b <sub>1</sub> =1.90
	<b>H</b> <sub>0</sub>   [001]						
2	<b>k</b> <sub>long</sub>   [100]	30.0	1.85	6.80×10 <sup>-3</sup>	$\frac{4}{3} \frac{b_1^2}{C_{11}K}$	0.586	b <sub>1</sub> =1.95
	<b>H</b> <sub>0</sub>   [100]						
3	<b>k</b> <sub>long</sub>   [100]	30.0	2.00	1.55×10 <sup>-3</sup>	$\frac{1}{3} \frac{b_1^2}{C_{11}K}$	0.685	b <sub>1</sub> =2.02
	<b>H</b> <sub>0</sub>   [001]						
4	<b>k</b> <sub>long</sub>   [110] or [11̄0]	11.5	2.00	1.74×10 <sup>-3</sup>	$\frac{1}{3} \frac{(b_1 \pm b_2)^2}{C_L K}$	0.685	b <sub>1</sub> ±b <sub>2</sub> =2.05
	<b>H</b> <sub>0</sub>   [001]						
5	<b>k</b> <sub>long</sub>   [101] or [1̄01]	11.5	1.90	0.292×10 <sup>-3</sup>	$\frac{1}{12} \frac{(b_1 \pm 2b_2)}{C_L K}$	0.620	b <sub>1</sub> ±2b <sub>2</sub> =1.66
	<b>H</b> <sub>0</sub>   [001]						
6	<b>k</b> <sub>trans</sub>   [101]	10.2	2.00	11.5×10 <sup>-3</sup>	$\frac{3}{4} \frac{b_1^2}{C'K}$	0.685	b <sub>1</sub> =2.11
	ε  [101] <b>H</b> <sub>0</sub>   [001]						
7	Eastman-AFMR under static uniaxial stress	...	...	...	...	0.866	b <sub>1</sub> =1.5±0.15
7'		...	...	...	...	...	b <sub>2</sub> =0.16±0.02
							b <sub>1</sub> =1.8±0.15
							b <sub>2</sub> =0.175±0.02

<sup>a</sup> T = 4.2 K.  
<sup>b</sup> K = M<sub>0</sub>H<sub>E</sub><sup>2</sup>/2H<sub>E</sub>, where M<sub>0</sub> = 305 G, H<sub>E</sub> = 8.9 × 10<sup>5</sup> Oe.  
<sup>c</sup> C<sub>11</sub> = 1.275 × 10<sup>12</sup> ergs/cm<sup>2</sup>, C' = 0.4266 × 10<sup>12</sup> ergs/cm<sup>2</sup>, and C<sub>L</sub> = 1.175 × 10<sup>12</sup> ergs/cm<sup>2</sup>.

3. Longitudinal Waves, **k**||[110], **H**<sub>0</sub> in (11̄0) Plane

The dependence on magnetic field of

$$C_L^* = \frac{1}{2}(C_{11} + C_{12} + 2C_{44})^*$$

for **H**<sub>0</sub>||[001], [111], and [110] is given in Fig. 3. Rows 4-7 of Table I give the theoretical results for C<sub>L</sub><sup>\*</sup> as determined by propagation along the four equivalent [110] axes.

For **H**<sub>0</sub>||[001] and **k**||[110] or [11̄0] (equivalent experimental situations) rows 4 and 5 of Table II apply. The difference in these two results is due to the assumption that **M** remains in the (11̄0) plane. However, since b<sub>2</sub> ≪ b<sub>1</sub>, the two expressions are qualitatively the same and agree with the data of Fig. 3. They are compared to the data in row 4 of Table IV. Comparison of row 4 with rows 1, 2, and 3 of Table IV confirms our conclusion from the previous paragraph that b<sub>2</sub> ≪ b<sub>1</sub>.

When **k**||[101] or [1̄01] and **H**<sub>0</sub> is again parallel to [001], rows 6 and 7 of Table II apply. Again equivalent experimental conditions yield different but similar theoretical results. The comparison with experimental data (not shown here) is given in row 5 of Table IV.

Application of **H**<sub>0</sub> along the [111] axis with propagation along the [110] or [101] axes results in a smooth

decrease in C<sub>L</sub><sup>\*</sup> with increasing H<sub>0</sub>. Rows 4 and 6 of Table III cover this case and give qualitatively different results for the reasons discussed above.

When the field is aligned parallel to the propagation direction (i.e., **H**<sub>0</sub>||**k**||[110]) there is little difference between the low- and high-field values of C<sub>L</sub><sup>\*</sup>; however, at H<sub>0</sub> ≈ 1 kOe there is an apparent discontinuous jump in C<sub>L</sub><sup>\*</sup>. This is a result of the mechanical resonance

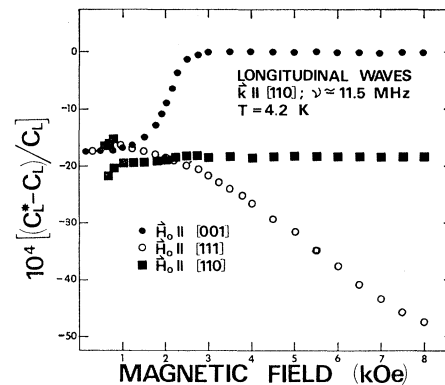


FIG. 3. Relative change in the elastic constant C<sub>L</sub><sup>\*</sup> = ½(C<sub>11</sub> + C<sub>12</sub> + 2C<sub>44</sub>)<sup>\*</sup> versus magnetic field for **H**<sub>0</sub> applied along three symmetry directions in the (110) plane; T = 4.2 K.

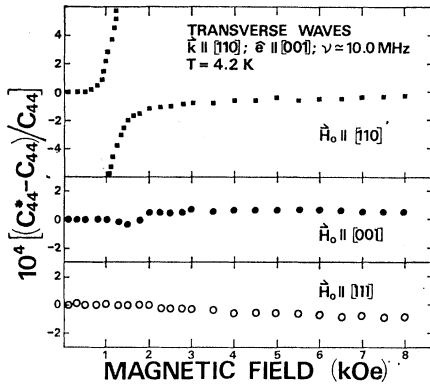


FIG. 4. Relative change in the elastic constant  $C_{44}^*$  versus magnetic field for  $H_0$  applied along three symmetry directions in the (110) plane;  $T=4.2$  K.

splitting into two peaks at this value of  $H_0$ ; one peak dominates at low fields and the other at high fields. This effect is most probably due to the existence of domains.<sup>13</sup>

4. Transverse Waves,  $k \parallel [110]$ ,  $\hat{e} \parallel [001]$ ,  $H_0$  in the  $(1\bar{1}0)$  Plane

The coupling constant for this case is again  $b_2$  [see rows 8 and 9 of Table I], thus indicating that the dependence on magnetic field is weak. This is demonstrated by the data of Fig. 4. Again, the initial conditions determine the result of the calculation, as shown by comparison of rows 8 and 9 of Table II which correspond to identical experimental conditions, i.e.,  $k \parallel [110]$  or  $[1\bar{1}0]$  and  $H_0 \parallel [001]$ .

The splitting of the mechanical resonance when  $H_0 \parallel [110] \parallel k$  and  $H_0 \approx 1$  kOe as seen in the top panel of Fig. 4 is similar to that discussed in the previous paragraph and is again attributed to domains. The bottom panel shows that  $C_{44}^*$  decreases slightly with increasing  $H_0$  for  $H_0 \parallel [111]$ .

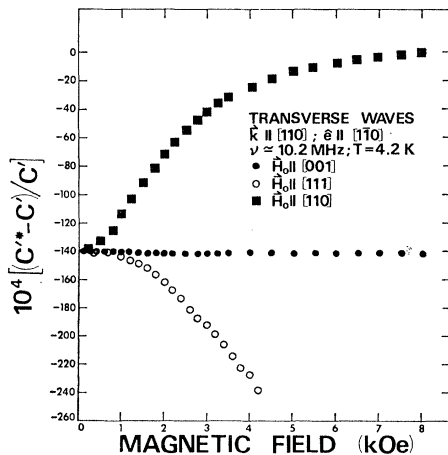


FIG. 5. Relative change in the elastic constant  $C'^* = \frac{1}{2}(C_{11} - C_{12})^*$  versus magnetic field for  $H_0$  applied along three symmetry directions in the  $(1\bar{1}0)$  plane;  $T=4.2$  K.

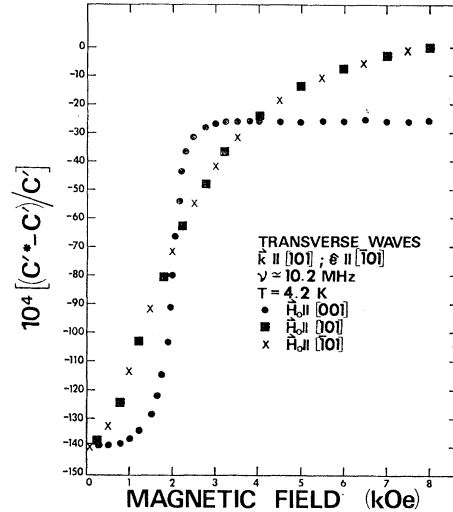


FIG. 6. Relative change in the elastic constant  $C'^* = \frac{1}{2}(C_{11} - C_{12})^*$  versus magnetic field for  $H_0$  applied along three symmetry directions in the (010) plane;  $T=4.2$  K.

5. Transverse Waves,  $k \parallel [110]$ ,  $\hat{e} \parallel [1\bar{1}0]$

Figures 5 and 6 show the magnetic field dependence of  $C'^* = \frac{1}{2}(C_{11} - C_{12})^*$  for several orientations of  $H_0$ . Rows 10 and 11 of Table I cover the four possible orientations of the directions of propagation with respect to the  $(1\bar{1}0)$  plane.

When  $H_0 \parallel [001]$  and  $k \parallel [110]$  or  $[1\bar{1}0]$ ,  $C'^*$  is seen (Fig. 5) to be independent of the magnitude of  $H_0$ . Such behavior is predicted by row 10 of Table II, which, for no obvious reason based on symmetry, yields identical results regardless of whether  $k \parallel [110]$  or  $k \parallel [1\bar{1}0]$ .

If the propagation direction is along the  $[101]$  or  $[1\bar{1}0]$  axes and  $H_0 \parallel [001]$  the expected behavior is given by rows 11 of Table II. Again the two theoretical results are identical and the good agreement with the experimental data (see Fig. 6) is shown in row 6 of Table IV.

Application of  $H_0$  along the  $[111]$  axis results in the expressions presented in rows 10 and 11 of Table III. These two expressions (for identical experimental situations) agree qualitatively (again because of our initial conditions on  $M_1^0$  and  $M_2^0$ , the exact expressions differ somewhat). Qualitative agreement with theory is shown by the data of Fig. 5.

In Fig. 6 it is shown that, for  $k \parallel [101]$  and  $H_0 \parallel [101] \parallel k$  or  $H_0 \parallel [101] \perp k$ , the experimental results are identical. By considering row 10 of Table I one sees that this must be the case.

B. Angular Dependence of Elastic Constants and Ultrasonic Attenuation at 4.2 and 77.4 K

We present here several representative sets of data for the relative change in the elastic constants and attenuation when a 7.5-kOe applied field is rotated with respect to the propagation vector  $k$  in specific crystallo-

graphic planes. The data show a remarkable difference between the behavior at 4.2 and 77.4 K.

1. Longitudinal Waves,  $k \parallel [001]$ ,  $H_0$  in  $(1\bar{1}0)$  Plane

Shown in Figs. 7(a) and 7(b), respectively, are the relative attenuation and relative elastic constant  $C_{11}$  for 10.6-MHz ultrasonic waves at 4.2 K. The data show a sharp minimum in  $\Delta C_{11}/C_{11}$  and a maximum in  $\alpha$  as  $H_0$  is rotated through the  $[111]$  direction. This behavior may not be explainable unambiguously on the basis of an equilibrium analysis. Considering the equilibrium orientation of the magnetization in high fields,<sup>12</sup> the magnetization remains in the  $(1\bar{1}0)$  plane for  $H_0$  between the  $[001]$  and  $[111]$  axes, i.e.,  $\psi \leq 54.7^\circ$ . For  $\psi \geq 54.7^\circ$  the magnetization abruptly flips out of the  $(1\bar{1}0)$  plane. The instability associated with this abrupt and irreversible behavior might be expected to lead to increased absorption and a "softening" of the lattice as observed.

The data for the identical experimental situation at 77.4 K is presented in Figs. 8(a) and 8(b). The gross difference in behavior at the two temperatures is difficult to understand since the same qualitative behavior is predicted at all temperatures by the theory outlined in Sec. II. It is perhaps worthwhile noting that the anisotropy constant  $K$ , which plays such an important role in these effects, is extremely small at  $T=77.4$  K.

2. Longitudinal Waves,  $k \parallel [001]$ ,  $H_0$  in  $(010)$  Plane

The relative elastic constants at 77.4 and 4.2 K for this case are given, respectively, in Figs. 9(a) and 9(b).

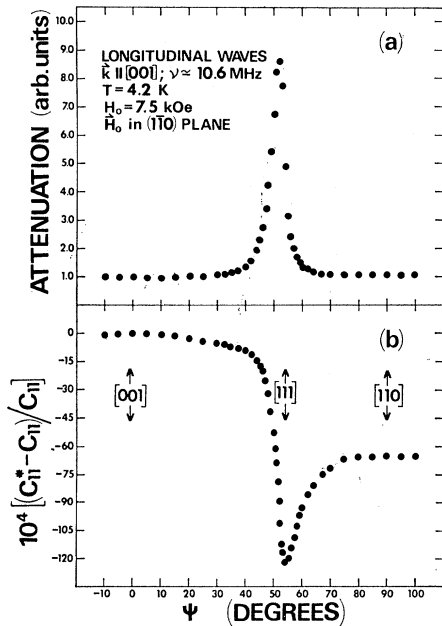


FIG. 7. Relative change in the attenuation (a) and the elastic constant  $C_{11}^*$  (b) versus orientation of the magnetic field ( $H_0=7.5$  kOe) in the  $(1\bar{1}0)$  plane for  $k_{\text{long}} \parallel [001]$ ;  $\nu \approx 10.6$  MHz;  $T=4.2$  K;  $\psi = \angle(H_0, [001])$ .

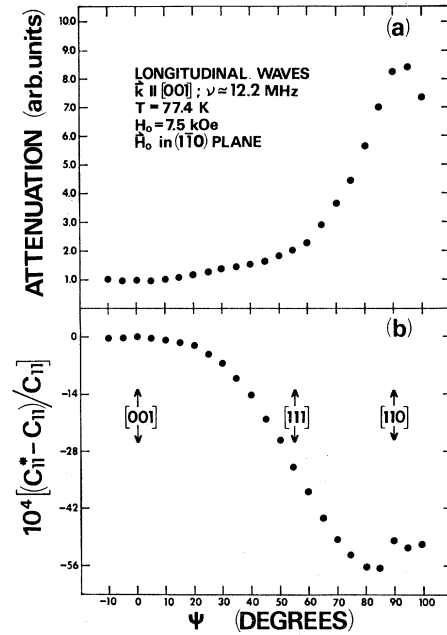


FIG. 8. Relative change in the attenuation (a) and the elastic constant  $C_{11}^*$  (b) versus orientation of the magnetic field ( $H_0=7.5$  kOe) in the  $(1\bar{1}0)$  plane for  $k_{\text{long}} \parallel [001]$ ;  $\nu \approx 12.2$  MHz;  $T=77.4$  K;  $\psi = \angle(H_0, [001])$ .

Several points of interest should be noted. The qualitative behavior at the two temperatures for  $H_0$  in the  $(010)$  plane is the same. The behavior at 4.2 K for  $H_0$  in the  $(010)$  and  $(1\bar{1}0)$  planes [see Figs. 9(b) and 7(b)] is qualitatively quite different. At 77.4 K the behavior is

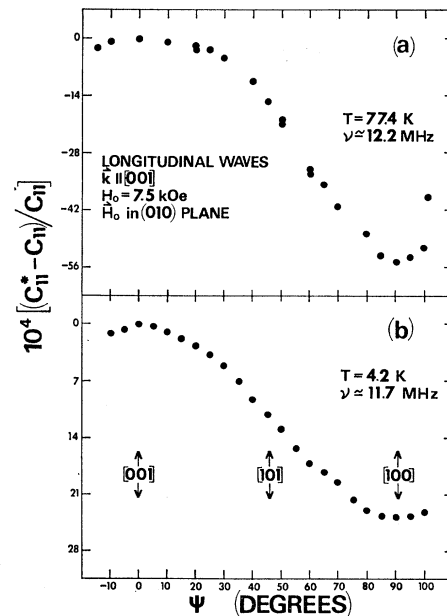


FIG. 9. Relative change in the elastic constant  $C_{11}^*$  versus orientation of the magnetic field ( $H_0=7.5$  kOe) in the  $(010)$  plane  $\psi = \angle(H_0, [001])$ . (a)  $T=77.4$  K,  $\nu \approx 12.2$  MHz; (b)  $T=4.2$  K,  $\nu \approx 11.7$  MHz.

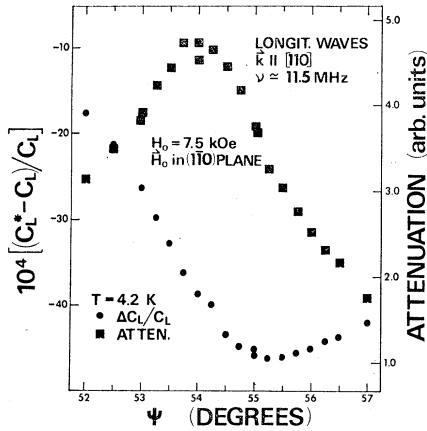


FIG. 10. Relative change in the attenuation and the elastic constant  $C_L^* = \frac{1}{2}(C_{11} + C_{12} + 2C_{44})^*$  versus orientation of the magnetic field ( $H_0 = 7.5$  kOe) in the  $(1\bar{1}0)$  plane;  $T = 4.2$  K,  $\nu \approx 11.5$  MHz;  $\psi = \angle(\mathbf{H}_0, [001])$ .

qualitatively and quantitatively the same [see Figs. 9(a) and 8(b)] regardless of in which of the two planes  $\mathbf{H}_0$  is rotated. This appears to indicate that the higher-temperature magnetic anisotropy effects are different than at the lower temperature.

3. Longitudinal Waves,  $\mathbf{k} \parallel [110]$ ,  $\mathbf{H}_0$  in  $(1\bar{1}0)$  Plane

The behavior of this mode at 4.2 K with  $\mathbf{H}_0$  in the  $(1\bar{1}0)$  plane is qualitatively similar to that shown in

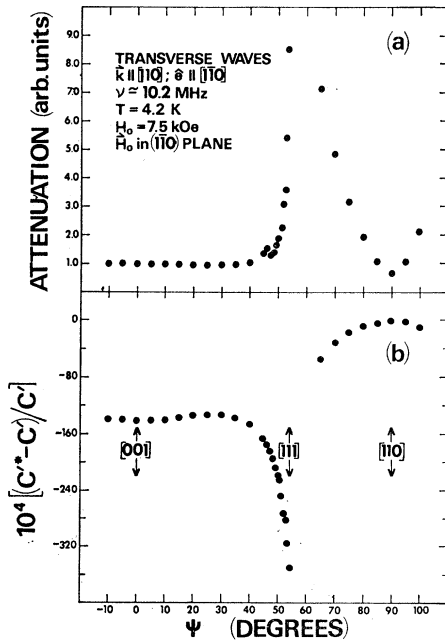


FIG. 11. Relative change in attenuation (a) and the elastic constant  $C^* = \frac{1}{2}(C_{11} - C_{12})^*$  (b) versus orientation of magnetic field ( $H_0 = 7.5$  kOe) in the  $(1\bar{1}0)$  plane.  $T = 4.2$  K,  $\nu \approx 10.2$  MHz,  $\psi = \angle(\mathbf{H}_0, [001])$ . Data for  $55^\circ < \psi < 65^\circ$  could not be obtained because of the high attenuation.

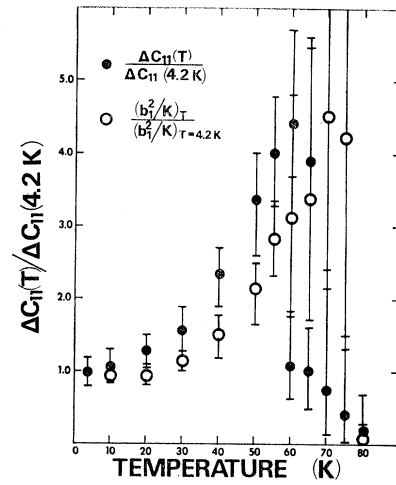


FIG. 12. Relative difference between the measured  $(C_{11}^*)$  and the pure elastic constant  $C_{11}$  versus temperature. The solid dots represent the quantity  $(C_{11}^*(T) - C_{11}(T)) / [C_{11}^*(4.2) - C_{11}(4.2)]$ ; the data are taken from Fig. 6 of I. The open circles represent the quantity  $(b_1^2/K)_T / (b_1^2/K)_{4.2\text{K}}$ ; the values of  $b_1(T)$  and  $K(T)$  are obtained from Refs. 4 and 21, respectively.

Figs. 7(a) and 7(b) for  $\mathbf{k} \parallel [001]$ . A detail of the relative behavior of the elastic constant and attenuation is the angular region near the  $[111]$  axis is given in Fig. 10. These data illustrate the interesting fact that the attenuation is a maximum for the magnetic field oriented about  $1\frac{1}{2}$  deg from the position at which the elastic constant is a minimum. This behavior is observed with each elastic mode for which the dependence on angle is sharp enough to allow the required angular resolution.

4. Transverse Waves,  $\mathbf{k} \parallel [110]$ ,  $\mathbf{e} \parallel [1\bar{1}0]$ ,  $\mathbf{H}_0$  in  $(110)$  Plane

In order to illustrate the qualitative difference between this transverse mode and the two longitudinal modes considered in Secs. IV B 1 and IV B 3 above, the behavior of the attenuation and  $C^*$  versus orientation of  $\mathbf{H}_0$  in the  $(1\bar{1}0)$  plane is shown in Fig. 11. Again, the minimum in the elastic constant is observed; data were not obtained in the angular region  $53^\circ < \theta < 65^\circ$  because of the extremely high attenuation. Note that for  $\mathbf{H}_0 \parallel [111]$  a difference in  $C^*$  of more than 3% from that for  $\mathbf{H}_0 \parallel [110]$  is measured.

C. Temperature Dependence

The temperature dependence of the difference,  $\Delta C_{ij} = C_{ij}^* - C_{ij}$ , between the measured and the pure elastic constant for a given elastic mode is given by the quantity  $b^2(T)/K(T)$ , where  $b(T)$  is the appropriate linear combination of the MECC  $b_1$  and  $b_2$ , and  $K(T)$  is the magnetocrystalline anisotropy constant.

In Fig. 12 the experimental values of  $\Delta C_{11}(T)/\Delta C_{11}(4.2 \text{ K})$  are plotted as a function of temperature (solid dots).<sup>20</sup> Using the experimental values of  $b_1(T)^4$  and  $K(T)^{21}$  the ratio  $[b_1^2/K]_T/[b_1^2/K]_{4.2 \text{ K}}$  has also been plotted in Fig. 12 (open circles). The errors for  $b_1^2(T)/K(T)$  were estimated from the scatter in the experimental data; they become rather large for  $T > 50 \text{ K}$ , since  $b_1(T)$  and  $K(T)$  become quite small as  $T$  approaches  $T_N$ . As discussed in I, there is also considerable uncertainty in the value of  $\Delta C_{11}(T)$  for  $T$  near 60 K because of the strong magnetoelastic coupling in this temperature region. Although there exists some systematic difference between the two sets of data, the agreement has to be considered satisfactory when the respective error bars are taken into consideration.

The effective elastic constants  $C_{11}^*$ ,  $C_L^*$ , and  $C'^*$  (whose ME component is dominated by the MECC  $b_1$ ) all show qualitatively the same behavior near  $T \approx 60 \text{ K}$ . The "anomaly" in  $C_{44}^*$  (whose ME component is dominated by the MECC  $b_2$ ) is so small that it can barely be observed experimentally. Since  $b_1$  is an order of magnitude larger than  $b_2$ , the anomaly in  $C_{44}^*$  is expected to be two orders of magnitude smaller than for the other modes as observed (see Figs. 6 and 7 of I).

The sensitivity of  $\Delta C_{ij} = C_{ij}^*(T) - C_{ij}(T)$  to  $K(T)$  demonstrates the important role played by the magnetic anisotropy in antiferromagnetic phenomena. In contrast, when treating rf ultrasonic propagation in a typical ferrimagnet, the anisotropy can be neglected.<sup>22</sup>

#### D. Magnetostriction in RbMnF<sub>3</sub>

Minimizing the free energy [Eq. (1)] with respect to the strains  $e_{ij}$ , the following expressions are obtained for the static strains:

$$e_{ii} = \frac{2b_1[C_{12} - (C_{11} + 2C_{12})\gamma_i^2]}{(C_{11} - C_{12})(C_{11} + 2C_{12})} \quad (18)$$

and

$$e_{ij} = -\frac{2b_2}{C_{44}}\gamma_i\gamma_j, \quad i \neq j \quad (19)$$

where the  $\gamma_i$  are the direction cosines of the equilibrium sublattice magnetization with respect to the crystal coordinate system, and we have made the approxima-

tion that  $\mathbf{M}_1^0 = -\mathbf{M}_2^0$ . The relative change in length of the specimen due to the spontaneous magnetic order in a direction defined by the direction cosines  $\beta_i$  is given by

$$\frac{\Delta l}{l_0} = \frac{-2b_1}{C_{11} - C_{12}} \sum_{i=x,y,z} \gamma_i^2 \beta_i^2 - \frac{2b_2}{C_{44}} (\gamma_x \gamma_y \beta_x \beta_y + \text{c.p.}) + \frac{2b_1 C_{12}}{(C_{11} - C_{12})(C_{11} + 2C_{12})}. \quad (20)$$

The length changes resulting from the reorientation of the sublattices due to the applied field  $\mathbf{H}_0$  can be calculated from Eq. (20). It is found that our use of Eq. (17) is justified because typically,  $\Delta l/l < 5 \times 10^{-6}$ . Since  $b(T)/C_{ij}(T)$  is a smooth monotonic function of temperature no anomaly in the magnetostriction is expected near  $T \approx 60 \text{ K}$  corresponding to the "anomaly" in the measured elastic constants  $C_{ij}^*(T)$ .

#### V. SUMMARY AND CONCLUSIONS

In this paper we have presented an experimental and theoretical study of the propagation of ultrasonic waves in the antiferromagnetic state of RbMnF<sub>3</sub>. It is found that the magnetic field dependence of the effective elastic constants can be understood on the basis of a model in which the effective magnetoelastic coupling is determined by the equilibrium orientation of the sublattice magnetization; the orientation is determined by the applied magnetic field.

For all cases considered in which the theoretical results are unique, they are in agreement with the experimental results, both quantitatively and qualitatively. The magnetoelastic coupling constants obtained in this way at  $T = 4.2 \text{ K}$  are

$$b_1 = 1.95 \pm 0.15 \times 10^6 \text{ ergs/cm}^3,$$

$$b_2 \leq 0.2 \pm 0.1 \times 10^6 \text{ ergs/cm}^3.$$

The anisotropy constant is found to be  $K = 0.62 \pm 0.06 \times 10^3 \text{ ergs/cm}^3$ . Eastman's values of  $K$ ,  $b_1$ , and  $b_2$  are given in row 7 of Table IV. In row 7' are given the values of  $b_1$  and  $b_2$  obtained from Eastman's data using our I values of the elastic constants at 4.2 K.<sup>1</sup>

The "anomalies" in the measured elastic constants  $C_{ij}^*$  observed previously<sup>1,2</sup> are readily explained on the basis of the present model.

In those experimental cases for which the orientation of the sublattice magnetization is not uniquely known

<sup>20</sup> The values of  $C_{11}^*(T) - C_{11}(T)$  are obtained from Fig. 6 of I.  
<sup>21</sup> M. J. Freiser, R. J. Joenk, P. E. Seiden, and D. T. Teaney, in *Proceedings of the International Conference on Magnetism, Nottingham, 1964* (The Institute of Physics and The Physical Society, London, 1965), p. 432.

<sup>22</sup> D. E. Eastman, *Phys. Rev.* **148**, 530 (1966).

the theory gives ambiguous results. A better knowledge of the state of the magnetization should enable one to obtain agreement with experiment in these instances. In addition, domain effects greatly complicate the analysis in some cases and are believed to cause the apparent discontinuous behavior shown in Figs. 3 and 4.

The gross qualitative differences in the magnetic field orientation dependence of the elastic constants at 4.2 and 77.4 K do not appear to be explainable on the basis of the present theory.

The peaks and absorption edges in the ultrasonic attenuation observed by Shapira and Zak<sup>23</sup> in the uniaxial antiferromagnet  $\text{MnF}_2$  in the neighborhood of the spin-flop transition apparently result from a process fundamentally different from that considered in the present paper for  $\text{RbMnF}_3$ . Tani<sup>24</sup> has proposed that at least some of the  $\text{MnF}_2$  results are caused by volume magnetostrictive coupling to the spin-wave instabilities which exist at the spin-flop transition. This mechanism need not be considered in the present experiments on  $\text{RbMnF}_3$  when  $\mathbf{H}_0 \parallel [001]$ . For this field orientation no instabilities exist, i.e., the magnetization is at equilibrium for all values of  $H_0$ , and there is no transition analogous to the spin-flop transition. For  $\mathbf{H}_0 \parallel [111]$  in  $\text{RbMnF}_3$  spin flopping and attendant instabilities may exist.<sup>3</sup>

#### ACKNOWLEDGMENT

Dr. R. W. H. Stevenson of the University of Aberdeen supplied the single-crystal specimens of  $\text{RbMnF}_3$  used in this study.

#### APPENDIX A: EQUILIBRIUM COORDINATE SYSTEMS

We define the equilibrium coordinate systems  $(\hat{x}', \hat{y}', \hat{z}')$  in which  $\mathbf{M}_1^0 \parallel \hat{z}'$ , and  $(\hat{x}'', \hat{y}'', \hat{z}'')$  in which  $\mathbf{M}_2^0 \parallel \hat{z}''$ , where  $\mathbf{M}_1^0$ , and  $\mathbf{M}_2^0$  represent the equilibrium sublattice magnetizations. The magnetization components  $M_{ij}$  in the crystal coordinate system  $(\hat{x}, \hat{y}, \hat{z})$  are expressed in terms of the components  $M_{ij'}$  or  $M_{ij''}$  in the equilibrium systems  $(\hat{x}', \hat{y}', \hat{z}')$  and  $(\hat{x}'', \hat{y}'', \hat{z}'')$ :

$$\begin{aligned} M_{1x} &= M_{1x'} \cos \theta_1 \cos \varphi_1 - M_{1y'} \sin \varphi_1 \\ &\quad + M_{1z'} \sin \theta_1 \cos \varphi_1, \\ M_{1y} &= M_{1x'} \cos \theta_1 \sin \varphi_1 + M_{1y'} \cos \varphi_1 \\ &\quad + M_{1z'} \sin \theta_1 \sin \varphi_1, \quad (\text{A1}) \\ M_{1z} &= -M_{1x'} \sin \theta_1 + M_{1z'} \cos \theta_1. \end{aligned}$$

The equations for  $\mathbf{M}_2$  are obtained by setting  $1 \rightarrow 2$  and  $(\hat{x}', \hat{y}', \hat{z}') \rightarrow (\hat{x}'', \hat{y}'', \hat{z}'')$ .

By substituting [Eq. (A1)] into Eqs. (2)–(6), the free-energy terms are written.

$$\begin{aligned} E_{\text{EX}} &= -\lambda \{ M_{1x} M_{2x} [\cos \theta_1 \cos \theta_2 \cos(\varphi_1 - \varphi_2) + \sin \theta_1 \sin \theta_2] + M_{1y} M_{2y} [\cos(\varphi_1 - \varphi_2)] \\ &\quad + M_{1z} M_{2z} [\sin \theta_1 \sin \theta_2 \cos(\varphi_1 - \varphi_2) + \cos \theta_1 \cos \theta_2] + M_{1x} M_{2y} [\cos \theta_1 \sin(\varphi_1 - \varphi_2)] - M_{1y} M_{2x} [\cos \theta_2 \sin(\varphi_1 - \varphi_2)] \\ &\quad + M_{1x} M_{2z} [\cos \theta_1 \sin \theta_2 \cos(\varphi_1 - \varphi_2) - \sin \theta_1 \cos \theta_2] + M_{1z} M_{2x} [\sin \theta_1 \cos \theta_2 \cos(\varphi_1 - \varphi_2) - \cos \theta_1 \sin \theta_2] \\ &\quad - M_{1y} M_{2z} [\sin \theta_2 \sin(\varphi_1 - \varphi_2)] + M_{1z} M_{2y} [\sin \theta_1 \sin(\varphi_1 - \varphi_2)] \}, \quad (\text{A2}) \end{aligned}$$

$$\begin{aligned} E_Z &= -\{ H_{0x} [M_{1x} \cos \theta_1 \cos \varphi_1 + M_{2x} \cos \theta_2 \cos \varphi_2 - M_{1y} \sin \varphi_1 - M_{2y} \sin \varphi_2 + M_{1z} \sin \theta_1 \cos \varphi_1 + M_{2z} \sin \theta_2 \cos \varphi_2] \\ &\quad + H_{0y} [M_{1x} \cos \theta_1 \sin \varphi_1 + M_{2x} \cos \theta_2 \sin \varphi_2 + M_{1y} \cos \varphi_1 + M_{2y} \cos \varphi_2 + M_{1z} \sin \theta_1 \sin \varphi_1 + M_{2z} \sin \theta_2 \sin \varphi_2] \\ &\quad + H_{0z} [-M_{1x} \sin \theta_1 - M_{2x} \sin \theta_2 + M_{1z} \cos \theta_1 + M_{2z} \cos \theta_2] \}, \quad (\text{A3}) \end{aligned}$$

$$\begin{aligned} E_A &= -(K/M^4) \{ (M_{1x}^2 M_{1z}^2 + M_{2x}^2 M_{2z}^2) [1 - \frac{3}{2} \sin^2 2\theta_1 (1 - \frac{1}{4} \sin^2 2\varphi_1)] + (M_{1y}^2 M_{1z}^2 + M_{2y}^2 M_{2z}^2) \\ &\quad \times [1 - \frac{3}{2} \sin^2 \theta_1 \sin^2 2\varphi_1] + \frac{1}{4} (M_{1z}^4 + M_{2z}^4) [\sin^2 2\theta_1 + \sin^4 \theta_1 \sin^2 2\varphi_1] + \frac{3}{4} (M_{1x} M_{1y} M_{1z}^2 - M_{2x} M_{2y} M_{2z}^2) \\ &\quad \times [\sin \theta_1 \sin 2\theta_1 \sin 4\varphi_1] + \frac{1}{2} (M_{1x} M_{1z}^3 + M_{2x} M_{2z}^3) [\sin 4\theta_1 + \sin^2 \theta_1 \sin 2\theta_1 \sin^2 2\varphi_1] \\ &\quad + \frac{1}{2} (M_{1y} M_{1z}^3 - M_{2y} M_{2z}^3) [\sin^3 \theta_1 \sin 4\varphi_1] \} \quad (\text{A4}) \end{aligned}$$

$$E_E = \frac{1}{2} C_{11} \sum_{j=x,y,z} e_{jj}^2 + \frac{1}{2} C_{44} (e_{xy}^2 + \text{c.p.}) + C_{12} (e_{xx} e_{yy} + \text{c.p.}) \quad (\text{A5})$$

<sup>23</sup> Y. Shapira and J. Zak, Phys. Rev. **170**, 503 (1968).

<sup>24</sup> K. Tani, Phys. Letters **26A**, 419 (1968).

$$\begin{aligned}
E_{ME} = & M_0^{-2} \{ [B_1(M_{1z}^2 + M_{2z}^2) - B_3 M_{1z} M_{2z}] \sin^2 \theta_1 \cos^2 \varphi_1 + [B_1(M_{1x} M_{1z} + M_{2x} M_{2z}) - \frac{1}{2} B_3 (M_{1x} M_{2z} + M_{1z} M_{2x})] \\
& \times \sin 2\theta_1 \cos^2 \varphi_1 - [B_1(M_{1y} M_{1z} - M_{2y} M_{2z}) - \frac{1}{2} B_3 (M_{1y} M_{2z} + M_{1z} M_{2y})] \sin \theta_1 \sin 2\varphi_1 \} e_{xx} \\
& + M_0^{-2} \{ [B_1(M_{1z}^2 + M_{2z}^2) - B_3 M_{1z} M_{2z}] \sin^2 \theta_1 \sin^2 \varphi_1 + [B_1(M_{1x} M_{1z} + M_{2x} M_{2z}) - \frac{1}{2} B_3 (M_{1x} M_{2z} + M_{1z} M_{2x})] \\
& \times \sin 2\theta_1 \sin^2 \varphi_1 + [B_1(M_{1y} M_{1z} - M_{2y} M_{2z}) - \frac{1}{2} B_3 (M_{1y} M_{2z} - M_{1z} M_{2y})] \sin \theta_1 \sin 2\varphi_1 \} e_{yy} \\
& + M_0^{-2} \{ [B_1(M_{1z}^2 + M_{2z}^2) - B_3 M_{1z} M_{2z}] \cos^2 \theta_1 - [B_1(M_{1x} M_{1z} + M_{2x} M_{2z}) - \frac{1}{2} B_3 (M_{1x} M_{2z} + M_{1z} M_{2x})] \\
& \times \sin 2\theta_1 \} e_{zz} + M_0^{-2} \{ [\frac{1}{2} B_2 (M_{1z}^2 + M_{2z}^2) - B_4 M_{1z} M_{2z}] \sin^2 \theta_1 \sin 2\varphi_1 + [\frac{1}{2} B_2 (M_{1x} M_{1z} + M_{2x} M_{2z}) \\
& - \frac{1}{2} B_4 (M_{1x} M_{2z} + M_{1z} M_{2x})] \sin 2\theta_1 \sin 2\varphi_1 + [B_2 (M_{1y} M_{1z} - M_{2y} M_{2z}) - B_4 (M_{1y} M_{2z} - M_{1z} M_{2y})] \\
& \times \sin \theta_1 \cos 2\varphi_1 \} e_{xy} + M_0^{-2} \{ [\frac{1}{2} B_2 (M_{1z}^2 + M_{2z}^2) - B_4 M_{1z} M_{2z}] \sin 2\theta_1 \cos \varphi_1 \\
& + [B_2 (M_{1x} M_{1z} + M_{2x} M_{2z}) - B_4 (M_{1x} M_{2z} + M_{1z} M_{2x})] \cos 2\theta_1 \cos \varphi_1 \\
& - [B_2 (M_{1y} M_{1z} - M_{2y} M_{2z}) - B_4 (M_{1y} M_{2z} - M_{1z} M_{2y})] \cos \theta_1 \sin \varphi_1 \} e_{xz} + M_0^{-2} \{ [\frac{1}{2} B_2 (M_{1z}^2 + M_{2z}^2) - B_4 M_{1z} M_{2z}] \\
& \times \sin 2\theta_1 \sin \varphi_1 + [B_2 (M_{1x} M_{1z} + M_{2x} M_{2z}) - B_4 (M_{1x} M_{2z} + M_{1z} M_{2x})] \cos 2\theta_1 \sin \varphi_1 \\
& + [B_2 (M_{1y} M_{1z} - M_{2y} M_{2z}) - B_4 (M_{1y} M_{2z} - M_{1z} M_{2y})] \cos \theta_1 \cos \varphi_1 \} e_{yz}. \quad (A6)
\end{aligned}$$

The primes denoting the equilibrium coordinate systems have been deleted for simplicity. Note that components  $H_{0i}$  ( $i=x, y, z$ ) of the dc field and the strains  $e_{ij}$  ( $i, j=x, y, z$ ) are still expressed with respect to the crystal coordinate system  $(\hat{x}, \hat{y}, \hat{z})$ . Third- and higher-order terms in the small quantities  $M_{ij}$  ( $i=1, 2; j=x, y$ ) and  $e_{ij}$  have been neglected (this is consistent with the linear approximation used in solving the equations of motion). In the expressions for  $E_A$  and  $E_{ME}$  the additional approximation that  $\varphi_2 = \varphi_1$  and  $\theta_2 = \theta_1 + \pi (\mathbf{M}_1^0 = -\mathbf{M}_2^0)$  has been made.

#### APPENDIX B: DEFINITION OF THE COEFFICIENTS IN EQS. (13)

The coefficients in Eqs. (13) are defined in terms of the material constants of the system, the propagation vector  $\mathbf{k}$ , and frequency  $\omega$  of the magnetoelastic modes and the magnetic field  $\mathbf{H}_0$ :

$$\begin{aligned}
\Gamma_{xx} = & -\rho\omega^2 + (C_{11} - 2b_1 \sin^2 \theta) k_x^2 + C_{44} (k_y^2 + k_z^2) - 2b_2 [\sin^2 \theta k_y + (\sin 2\theta/\sqrt{2}) k_z] k_x, \\
\Gamma_{yy} = & -\rho\omega^2 + (C_{11} - 2b_1 \sin^2 \theta) k_y^2 + C_{44} (k_x^2 + k_z^2) - 2b_2 [\sin^2 \theta k_x + (\sin 2\theta/\sqrt{2}) k_z] k_y, \\
\Gamma_{zz} = & -\rho\omega^2 + (C_{11} - 4b_1 \cos^2 \theta) k_z^2 + C_{44} (k_x^2 + k_y^2) - 2b_2 (\sin 2\theta/\sqrt{2}) (k_x + k_y) k_z, \\
\Gamma_{xy} = & (C_{12} + C_{44} - 2b_1 \sin^2 \theta) k_x k_y - 2b_2 [\sin^2 \theta k_x + (\sin 2\theta/\sqrt{2}) k_z] k_x, \\
\Gamma_{xz} = & (C_{12} + C_{44} - 4b_1 \cos^2 \theta) k_x k_z - 2b_2 (\sin 2\theta/\sqrt{2}) (k_x + k_y) k_x, \\
\Gamma_{yx} = & (C_{12} + C_{44} - 2b_1 \sin^2 \theta) k_x k_y - 2b_2 [\sin^2 \theta k_y + (\sin 2\theta/\sqrt{2}) k_z] k_y, \\
\Gamma_{yz} = & (C_{12} + C_{44} - 4b_1 \cos^2 \theta) k_y k_z - 2b_2 (\sin 2\theta/\sqrt{2}) (k_x + k_y) k_y, \\
\Gamma_{zx} = & (C_{12} + C_{44} - 2b_1 \sin^2 \theta) k_x k_z - 2b_2 [\sin^2 \theta k_y + (\sin 2\theta/\sqrt{2}) k_z] k_z, \\
\Gamma_{zy} = & (C_{12} + C_{44} - 2b_1 \sin^2 \theta) k_y k_z - 2b_2 [\sin^2 \theta k_x + (\sin 2\theta/\sqrt{2}) k_z] k_z,
\end{aligned} \quad (B1)$$

$$\begin{aligned}
a = & -i\omega, \\
b = & a_{12} - \omega_E - \omega_0 \cos \varphi, \\
c = & a_{21} + \omega_E + \omega_0 \cos \varphi, \\
d = & -\omega_E, \\
e = & -\omega_E \cos 2t \simeq -\omega_E + \frac{1}{2} (\omega_0^2/\omega_E) \sin^2 \varphi, \\
f = & -a_{12} + \omega_E - \omega_0 \cos \varphi, \\
g = & -a_{21} - \omega_E + \omega_0 \cos \varphi,
\end{aligned} \quad (B2)$$

where

$$a_{12} = \frac{3}{2} \omega_A (1 - \frac{7}{2} \sin^2 \theta + \frac{3}{2} \sin^4 \theta), \quad a_{21} = -\frac{3}{2} \omega_A (1 - \frac{1}{2} \sin^2 \theta + 6 \sin^4 \theta) \quad (B3)$$

and

$$\omega_0 = -\gamma H_0, \quad \omega_E = -\gamma H_E, \dots, \text{ etc.} \quad (B4)$$

Finally, the magnetoelastic torques and stresses are given in terms of the components

$$\begin{aligned}
 t_{11} &= b_1 \sin\theta k_x + b_2(\sqrt{\frac{1}{2}}) \cos\theta k_z, \\
 t_{12} &= -b_1 \sin\theta k_y - b_2(\sqrt{\frac{1}{2}}) \cos\theta k_z, \\
 t_{13} &= b_2(\sqrt{\frac{1}{2}}) \cos\theta(k_x - k_y), \\
 t_{21} &= b_1 \times \frac{1}{2} \sin 2\theta k_x + b_2 \times \frac{1}{2} \sin 2\theta k_y + b_2(\sqrt{\frac{1}{2}}) \cos 2\theta k_z, \\
 t_{22} &= b_1 \times \frac{1}{2} \sin 2\theta k_y + b_2(\sqrt{\frac{1}{2}}) \cos\theta k_z + b_2 \times \frac{1}{2} \sin 2\theta k_x, \\
 t_{23} &= -b_1 \sin 2\theta k_z + b_2(\sqrt{\frac{1}{2}}) \cos 2\theta(k_x + k_y).
 \end{aligned} \tag{B5}$$

The  $S_m^\pm$  of Eqs. (13) are defined by

$$S_m^\pm = [3K \sin 2\theta (1 - \frac{3}{2} \sin^2\theta) \pm M_0 H_0 \sin\varphi] k_m, \quad m = x, y, z. \tag{B6}$$

### Lorenz Number for Metals with Magnetic Impurities\*

SANG BOO NAM AND MARTIN S. FULLENBAUM

*Department of Physics, University of Virginia, Charlottesville, Virginia 22903*

(Received 12 May 1969)

A simple formula for the electronic thermal and dc electrical conductivities has been obtained by expanding the  $t$  matrix. The result is applied to get the Lorenz number. We found that the Lorenz number for metals with magnetic impurities has a maximum at a certain temperature.

**I**N this paper we show that one can calculate algebraically the electronic thermal and dc electrical conductivities for metals by expanding the  $t$  matrix in terms of the frequency variable.

In general, the thermal ( $K$ ) and dc electrical ( $\sigma$ ) conductivities for metals may be written as<sup>1</sup>  $K = ATI_2$  and  $\sigma = BI_0$ , where

$$I_n = \left(\frac{1}{2T}\right)^{n+1} \int_0^\infty d\omega \omega^n \Phi(\omega, T) \operatorname{sech}^2 \frac{\omega}{2T}. \tag{1}$$

The function  $\Phi$  is given in the usual way by the average value of the product of the square of the group velocity and the relaxation time over the equal-energy surface with an appropriate density of states. In most cases, the group velocity and the appropriate density of states are almost constant. The main variation in  $\Phi$  comes from the relaxation time which in turn is given by the imaginary part of the  $t$  matrix:

$$(2\tau)^{-1} = \operatorname{Im}t.$$

By inspecting the integrand in Eq. (1), we see that the factor  $\operatorname{sech}^2(\omega/2T)$  makes the integral converge uni-

formly. We may expand  $\Phi$  in terms of  $\omega/2T = x$ :

$$\begin{aligned}
 \Phi(\omega, T) &= \sum_{m, n=0} \left\{ \theta(R_{m+1} - x) \theta(x - R_m) \right. \\
 &\quad \left. \times \left[ a(n, m, T) \left(\frac{x}{R_{m+1}}\right) + b(n, m, T) \left(\frac{R_m}{x}\right)^n \right] \right\}, \tag{2}
 \end{aligned}$$

where  $\theta(x) = 1$  for  $x > 0$ ,  $\theta(x) = 0$  for  $x < 0$ , and  $R_m$  are the radii of convergence of the expansion. In practice, only even-power terms contribute in Eq. (2), since  $\operatorname{Im}t(\omega) = \operatorname{Im}t(-\omega)$ . Inserting Eq. (2) into Eq. (1), we obtain  $K$  and  $\sigma$ :

$$K = \sum_{m, n} [a(2n, m, T) S(2n+2, m) R_{m+1}^2 + b(2n, m, T) U(2n-2, m) R_m^2], \tag{3}$$

$$\sigma = \sum_{m, n} [a(2n, m, T) S(2n, m) + b(2n, m, T) U(2n, m)], \tag{4}$$

where

$$R_{m+1}^n S(n, m) = \int_{R_m}^{R_{m+1}} x^n \operatorname{sech}^2 x dx = R_m^n U(-n, m). \tag{5}$$

For metals with magnetic impurities described by the  $s$ - $d$  interaction, the imaginary part of the  $t$  matrix may be written

$$(2\tau)^{-1} = (\operatorname{Im}t)_{J=0} + C(\operatorname{Im}t)_J,$$

where  $J$  is the coupling constant of the  $s$ - $d$  interaction,

\* Work supported in part by the U. S. Air Force under contract No. AFSOR-1138-66 and the Center for Advanced Studies under NSF Grant No. NSF-GU-1581.

<sup>1</sup> N. H. Mott and H. Jones, *The Theory of the Properties of Metals and Alloys* (Dover Publications, Inc., New York, 1958), p. 306; S. B. Nam, *Phys. Rev.* **156**, 470 (1967), Eq. (5.5), Ref. 40. [ $\Gamma(\omega)$  is proportional to the inverse of the relaxation time.]